Chaos, Solitons and Fractals 186 (2024) 115286

Contents lists available at ScienceDirect

Chaos, Solitons and Fractals

journal homepage: www.elsevier.com/locate/chaos

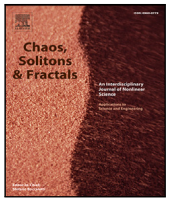

A simple model of global cascades in signed networks

Xingfu Ke, Youjin Wen, Hao Yu *, Fanyuan Meng *

Research Center for Complexity Sciences, Hangzhou Normal University, Hangzhou, 311121, Zhejiang, China

ARTICLE INFO

Keywords:
Signed networks
Negative links
Information cascade
Threshold
Phase transition

ABSTRACT

Negative relationships play a crucial role in the diffusion of information across social networks. To explore this phenomenon, we introduce a threshold model for information cascades in signed networks, which includes a weighted parameter $\alpha \in (-\infty, 1]$ to represent the impact of negative links, causing decay or negative influence. Using rigorous mean-field analysis, we identify the conditions that enable global cascades. Interestingly, we find that negative α results in the same cascade conditions as $\alpha = 0$. Furthermore, with negative α, the relationship between average degree and cascade size forms a bell-shaped curve, leading to second-order phase transitions at both low and high average degrees. These findings are consistent across random networks with Poisson and scale-free degree distributions. Overall, this research provides a theoretical framework for understanding the effects of negative connections on information diffusion in social networks, offering important insights into cascade dynamics and practical strategies for managing information dissemination in real-world contexts.

1. Introduction

In the contemporary world, individuals traverse a maze of intricate social relationships, facilitated by the pervasive presence of online platforms and digital communication tools [1–3]. These social networks, burgeoning from the intricate fabric of human societies, serve not only as arenas for social interaction but also as indispensable conduits for the rapid information diffusion, where ideas, opinions, and behaviors cascade across global populations [4–7]. Consequently, comprehending the mechanisms underpinning information cascade within these networks is imperative for predicting social trends and effectively managing the information diffusion [8–10].

The diffusion process is shaped by myriad factors, including network structure, content characteristics, user attributes, and relationship strengths. Network topology, for instance, influences the speed and reach of diffusion, with densely connected clusters fostering rapid diffusion while sparse connections may impede diffusion [11–13]. Meanwhile, the nature of the information itself, whether it is emotionally charged, true or false, or aligns with pre-existing beliefs, significantly affects its likelihood of being shared and adopted [14–16]. Moreover, individual attributes play a pivotal role in shaping information diffusion dynamics. Factors such as social influence, homophily, and opinion leaders influence the spread of information, creating cascades of adoption or resistance within the network [17–20]. Furthermore, considering the strength of social relationships, threshold-based models on weighted networks have been proposed to analyze information cascade processes [21,22].

Nevertheless, the type of social relationships can be diverse, encompassing not only positive bonds indicative of friendship or collaboration but also negative links stemming from rivalry or conflict [23–26]. Conventional models of information diffusion often oversimplify this aspect, while signed networks, characterized by the coexistence of positive and negative links, furnish an alternative framework for comprehending information diffusion [27–29].

To gain a deeper understanding of the intricate interplay between positive and negative relationships in information diffusion, our study builds upon previous research by explicitly incorporating both types of links into the model [30,31]. In contrast to the approach in [32], which focuses on the complete obstruction of information cascades by negative links, assuming that information propagates solely through positive links, our research introduces a weighted parameter $\alpha \in (-\infty, 1]$. This parameter allows us to modulate the influence of negative links on information adoption. By adjusting α, we explore a wide range of scenarios, from scenarios where information sources are completely blocked along negative links to scenarios where both positive and negative links are considered equally. This refined approach sheds light on how mixed ties comprehensively influence the dynamics of information cascades.

We designate a fraction of initially active seed nodes as focal points for initiating cascading effects. By scrutinizing the activation processes of nodes in response to both positive and negative links, we aim to elucidate the underlying mechanisms that govern information cascades in signed networks. Our model offers a versatile framework for

* Corresponding authors.
E-mail addresses: yuu_hao@outlook.com (H. Yu), fanyuan.meng@hotmail.com (F. Meng).

https://doi.org/10.1016/j.chaos.2024.115286
Received 11 May 2024; Received in revised form 18 June 2024; Accepted 11 July 2024
Available online 20 July 2024

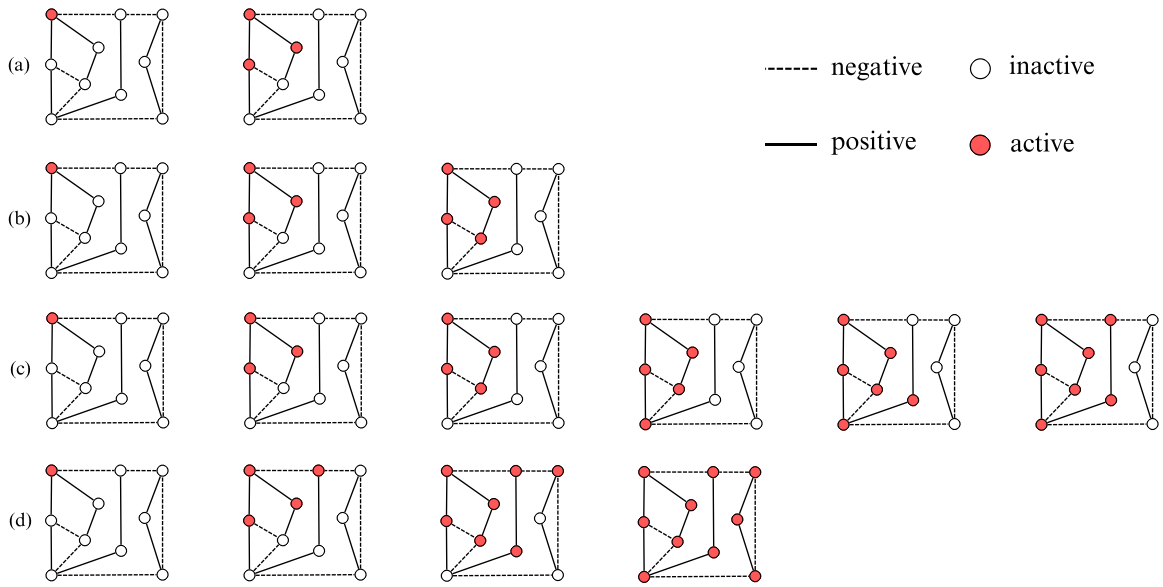

Fig. 1. The depiction illustrates information cascades for different weighted parameters α in a signed network with $N = 10$, $\rho_0 = 0.1$, and $\phi = 0.3$. Dashed lines signify negative links, while solid lines denote positive links. Inactive states are represented by white circles, while active states are highlighted in red. The settings are as follows: (a) $\alpha = -0.5$; (b) $\alpha = 0$; (c) $\alpha = 0.5$; (d) $\alpha = 1$.

analyzing cascade dynamics across diverse network topologies, initial conditions and link strengths. It enables us to simulate information diffusion through networks that realistically represent both supportive and adversarial relationships, thus providing a more accurate portrayal of the intricate dynamics observed in real-world social networks.

2. Model

We construct a random network of size N, where the degree of each node, denoted by k, follows a distribution p_k with an average degree $\langle k \rangle$. To develop a random signed network, we assign each link a sign: positive with probability $\eta \in [0, 1]$, and negative with probability $1 - \eta$. Initially, a fraction ρ_0 of seed nodes (i.e., seed size) are designated as active, representing early adopters of information.

The transition of a node from an inactive to an active state is governed by the condition

$$\frac{m_p + \alpha m_n}{k} > \phi, \tag{1}$$

where $\phi \in [0, 1]$ is the threshold that determines when a node shifts from being inactive to active. In this equation, m_p denotes the number of active nodes connected via positive links, and m_n represents the number of active nodes connected via negative links.

The parameter $\alpha \in (-\infty, 1]$ quantifies the influence of each active node connected by a negative link on the activation of a given node within the network. A positive α implies that negative links have a reduced effect on activation, while a negative α suggests an inhibitory effect of negative links on activation.

The information cascade process continues until no further nodes can be activated. In our model, the primary focus is on the average fraction of active nodes, referred to as the average cascade size ρ.

It is noteworthy that when $\alpha = 1$ (indicating equal weighting of contributions from active nodes through both positive and negative links) or $\eta = 1$ (indicating that all links are positive), our model reduces to the one proposed by [31].

Fig. 1 offers a visual depiction of the intricate dynamics of information cascades within a signed network with size $N = 10$, commencing from a single seed node. Central to this understanding is the pivotal role played by the weighted parameter α, which essentially determines the degree to which negative links hinder the diffusion of activation across the network. In case (a), where α is set to -0.5, the negative links exhibit a suppressive effect on the adoption of information. This is reflected in the final cascade size, which amounts to $\rho = 3/10$ (0.3), indicating that only a minority of nodes are activated. In contrast, case (b) with $\alpha = 0$ indicating an absence of any influence exerted by negative links. This leads to a slight increase in the cascade size, with a final cascade size of $\rho = 4/10$ (0.4). As we transition to case (c), characterized by $\alpha = 0.5$, we observe a more significant expansion in the cascade. Here, the negative links begin to exhibit a lesser inhibitory effect, enabling a broader diffusion of activation. Consequently, the cascade culminates in a cascade size of $\rho = 7/10$ (0.7), indicating a substantial increase in the number of activated nodes. Finally, in case (d), where α is set to 1, our model aligns with the seminal framework introduced by [31]. Here, both positive and negative links contribute equally to the activation process. This symmetry in link influence leads to the maximization of the cascade, ultimately resulting in the activation of all nodes and attaining a cascade size of $\rho = 1$.

3. Results

3.1. The cascade size

The average cascade size ρ can be derived using the following expression

$$\begin{aligned}\rho =& \rho_0 + (1 - \rho_0) \sum_{k=1}^{\infty} p_k \sum_{k_p=0}^{k} \binom{k}{k_p} \eta^{k_p} (1 - \eta)^{k - k_p} \\ & \times \sum_{m_p=0}^{k_p} \binom{k_p}{m_p} q_\infty^{m_p} (1 - q_\infty)^{k_p - m_p} \\ & \times \sum_{m_n=0}^{k-k_p} \binom{k - k_p}{m_n} q_\infty^{m_n} (1 - q_\infty)^{k - k_p - m_n} F\left(\frac{m_p + \alpha m_n}{k}\right),\end{aligned} \tag{2}$$

where q_∞ is the fixed point of the recursive equation

$$q_{n+1} = \rho_0 + (1 - \rho_0) G(q_n), \tag{3}$$

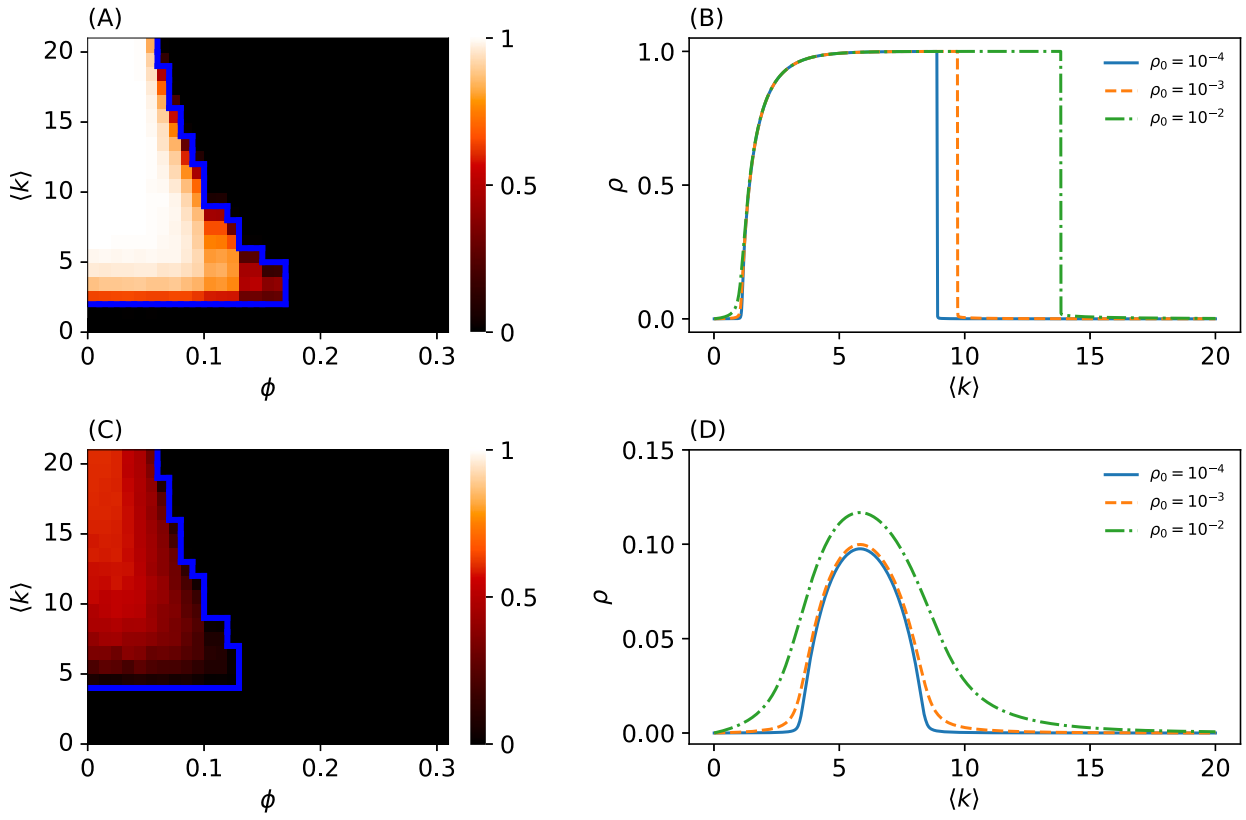

Fig. 2. The figure illustrates the cascade windows within the $(\phi, \langle k \rangle)$ planes and explores the relationship between the average cascade size ρ and the average degree $\langle k \rangle$ for different seed sizes ρ_0. The network employs a Poisson degree distribution $p_k = \frac{e^{-\langle k \rangle}\langle k \rangle^k}{k!}$. Panels (A) and (C) depict ρ color-coded and averaged over 10^3 realizations across varying ϕ and $\langle k \rangle$. Here, $N = 10^4$, $\eta = 0.3$, $\rho_0 = 10^{-4}$, and two scenarios are considered: $\alpha = 0.5$ (Panel A) and $\alpha = -0.5$ (Panel C). The solid blue line delineates an analytical approximation of the boundaries of global cascade windows. This line encloses the window where the condition outlined in Eq. (9) is satisfied. Panels (B) and (D) present the values of ρ at $\phi = 0.1$, derived from Eq. (2), represented by lines for $\alpha = 0.5$ (Panel B) and $\alpha = -0.5$ (Panel D) respectively. (For interpretation of the references to color in this figure legend, the reader is referred to the web version of this article.)

with $q_0 = \rho_0$, and the nonlinear equation G is defined by

$$G(q) = \sum_{k=1}^{\infty} \frac{kp_k}{\langle k \rangle} \sum_{k_p=0}^{k-1} \binom{k-1}{k_p} \eta^{k_p} (1-\eta)^{k-1-k_p} \sum_{m_p=0}^{k_p} \binom{k_p}{m_p} q^{m_p} (1-q)^{k_p - m_p} \times \sum_{m_n=0}^{k-1-k_p} \binom{k-1-k_p}{m_n} q^{m_n} (1-q)^{k-1-k_p-m_n} F\left(\frac{m_p + \alpha m_n}{k}\right). \tag{4}$$

Here $F(x)$ is a response function which is expressed as

$$F(x) = \begin{cases} 1 & \text{if } x > \phi, \\ 0 & \text{otherwise.} \end{cases} \tag{5}$$

Conceptually, the random network can be envisioned as a tree structure. The topmost level comprises a single node with a degree of k, connected to k neighbors at the subsequent level. Each of these connected nodes, in turn, is linked to $k-1$ neighbors at the next lower level, following a degree distribution denoted as $p'_k = \frac{kp_k}{\langle k \rangle}$. To ascertain the final fraction ρ of active nodes, we assign levels to the tree, with the bottom level labeled as $n = 0$ and the top node situated at level $n \to \infty$. Here, q_n denotes the conditional probability of a node at level n being active, given that the node at level $n+1$ is inactive. Considering the probability p'_k, the chosen node at level n has k neighbors: one being its parent node at level $n+2$, and the remaining $k-1$ being its children at level n. Consequently, the probability of having k_p positive links can be expressed as $\binom{k-1}{k_p}\eta^{k_p}(1-\eta)^{k-1-k_p}$. Furthermore, the probability of having m_p out of k_p active nodes and m_n out of $k-1-k_p$ active nodes can be computed as $\binom{k_p}{m_p}q^{m_p}(1-q)^{k_p-m_p}$ and $\binom{k-1-k_p}{m_n}q^{m_n}(1-q)^{k-1-k_p-m_n}$, respectively. Thus the activation of the chosen node can unfold in two scenarios: either it becomes a seed node, or it remains initially inactive with a probability of $1-\rho_0$ and becomes active due to the influence of active neighbors. This derivation leads to the recursive Eq. (3). Similarly, the probability governing the single node at the top level can be expressed using Eq. (2).

3.2. The cascade condition

The cascade condition serves as a crucial determinant of the occurrence of global cascades within the network. Expressing the equation $G(q)$ as a polynomial of the form $\sum_{l=0} C_l q^l$, with coefficients denoted as

$$C_l = \sum_{k=l+1}^{\infty} \frac{kp_k}{\langle k \rangle} \sum_{k_p=0}^{k-1} \binom{k-1}{k_p} \eta^{k_p} (1-\eta)^{k-1-k_p} \times \sum_{c=0}^{l} \binom{l}{c} \sum_{m_p=0}^{c} \binom{k_p}{c} \binom{c}{m_p} (-1)^{c+m_p} \times \sum_{m_n=0}^{l-c} \binom{k-1-k_p}{l-c} \binom{l-c}{m_n} (-1)^{l-c-m_n} F\left(\frac{m_p + \alpha m_n}{k}\right). \tag{6}$$

We introduce the equation $h(q)$ defined as

$$h(q) = \rho_0 + (1-\rho_0)G(q) - q. \tag{7}$$

Neglecting the higher-order term $O(q^2)$, we approximate $h(q)$ as

$$h(q) \approx \rho_0 + (1-\rho_0)(C_0 + C_1 q) - q. \tag{8}$$

Therefore, a global cascade occurs under the condition $(1-\rho_0)C_1 > 1$, as this ensures that q_n increases with n, at least initially. Utilizing

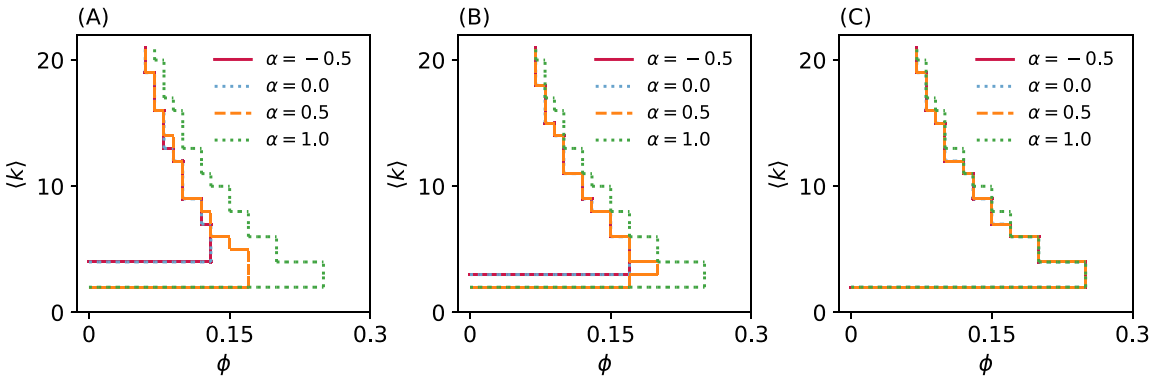

Fig. 3. The figure illustrates cascade windows within the $(\phi, \langle k \rangle)$ planes for different values of α, varying the fraction of positive links η, and using a seed size $\rho_0 = 10^{-3}$. The network follows a Poisson degree distribution $p_k = \frac{e^{-\langle k \rangle}\langle k \rangle^k}{k!}$. Panels (A), (B), and (C) correspond to different values of η: (A) $\eta = 0.3$, (B) $\eta = 0.5$, and (C) $\eta = 0.8$. The solid lines delineate the boundary of the global cascade window, determined by Eq. (9).

Eq. (6), we can derive the cascade condition

$$\sum_{k=1}^{\infty} \frac{k(k-1)p_k}{\langle k \rangle} \left[\eta F\left(\frac{1}{k}\right) + (1-\eta) F\left(\frac{\alpha}{k}\right) - F(0) \right] > \frac{1}{1-\rho_0}. \tag{9}$$

Notably, when the fraction of positive links $\eta = 1$ or the weighted parameter $\alpha = 1$, the formula simplifies to the cascade condition previously derived in [31] as

$$\sum_{k=1}^{\infty} \frac{k(k-1)p_k}{\langle k \rangle} \left[F\left(\frac{1}{k}\right) - F(0) \right] > \frac{1}{1-\rho_0}. \tag{10}$$

3.3. The cascade window

In Fig. 2, the color-coded visualization across the $(\phi, \langle k \rangle)$ parameter space in Panels (A,C) provides a profound understanding of the information cascade size. The cascade condition, formulated in Eq. (9), clearly outlines the boundary within which global cascades can emerge, denoted by the solid blue line. Panel (B) highlights the significant influence of the average degree $\langle k \rangle$ on the average cascade size ρ. For $\alpha = 0.5$, as $\langle k \rangle$ increases, a second-order phase transition in ρ is observed upon surpassing a critical threshold $\langle k \rangle_c^{II}$. This transition signifies the emergence of global cascades, followed by ρ gradually approaching 1. However, beyond a subsequent critical point $\langle k \rangle_c^{I}$, indicative of an even more densely connected network regime, a pronounced first-order phase transition takes place. Here, ρ undergoes a sudden drop to zero, indicating the potential impediment of information cascades in overly dense network environments. In contrast, for $\alpha = -0.5$ in Panel (D), the dynamics of the cascade size ρ exhibit a distinctly different pattern, resembling a bell-shaped curve. Specifically, as $\langle k \rangle$ increases, a second-order phase transition occurs with a critical point at $\langle k \rangle_{c2}^{II}$. The average cascade size ρ gradually attains a peak value at approximately $\langle k \rangle = 6$. Finally, another second-order phase transition occurs with a critical point at $\langle k \rangle_{c1}^{II}$, where the value of ρ decreases to zero.

In Fig. 3, variations in cascade windows within the $(\phi, \langle k \rangle)$ planes are displayed for different weighted parameters α. The panels illustrate how increasing α broadens the cascade window, as evident across the different panels distinguished by varying η values. It is notable that when α is set to -0.5 or 0, the cascade window remains identical. This occurs because the term $F\left(\frac{\alpha}{k}\right)$ in Eq. (9) evaluates to zero for all $\alpha \leq 0$, effectively leading to no distinction in the conditions that determine the global cascade window.

3.4. The complementary cascade size

The critical points $\rho_{0,c}$ and q_c are determined by satisfying the following conditions

$$\begin{cases} \frac{\partial h}{\partial q}(\rho_{0,c}, q_c) = 0, \\ h(\rho_{0,c}, q_c) = 0. \end{cases} \tag{11}$$

The graphical solutions of Eq. (7) across varied values of α within a random network are presented in Fig. 4. The constants $\langle k \rangle = 4$, $\eta = 0.2$, and $\phi = 0.334$ are maintained, while exploring different ρ_0 values.

Fig. 4 depicts the solutions of $h(\rho_0, q) = 0$ by varying the seed size ρ_0 for $\alpha = 0.5$ and $\alpha = 1$, respectively. Panel (A) demonstrates that for a lower value of α, specifically $\alpha = 0.5$, the solution is straightforward: regardless of the value of ρ_0, only a single solution is observed. Conversely, Panel (B) reveals a more intricate scenario for a higher value of α, such as $\alpha = 1$. Here, the behavior of the system changes significantly. For larger values of ρ_0, the curve can become tangent to the horizontal axis with multiple solutions, indicating that the system can undergo a phase transition. Specifically, a first-order percolation transition point is identified at $\rho_{0,c} \approx 0.104$. At this critical point, the parameter q experiences a sudden transition from q_{c1} to q_{c2}. This abrupt change characterizes a discontinuous transition in the complementary cascade size $(\rho - \rho_0)/(1-\rho_0)$, marking a significant shift in the system's state.

Fig. 5 provides insights into the impact of the initial seed size ρ_0 on the complementary cascade size $(\rho - \rho_0)/(1-\rho_0)$ across different parameters. The analytical results derived from Eq. (2) are represented by lines, while simulation outcomes are depicted by data points. The alignment between analytical predictions and simulation results underscores the model's accuracy in capturing information diffusion dynamics within random networks.

In Panel (A), for small values of η, the curve corresponding to $\alpha = 1$ exhibits a first-order phase transition, evidenced by a sudden increase in cascade size as ρ_0 crosses a critical point. Conversely, curves associated with lower α values (e.g., $\alpha = 0$ or $\alpha = 0.5$) demonstrate gradual growth as ρ_0 increases.

As η increases, shown in Panel (B) and further intensified in Panel (C), the cascade speed escalates gradually. Consequently, curves associated with lower α values can also manifest a first-order phase transition, as observed in Panel (C) for $\alpha = 0$.

3.5. The network structure

To explore how network structure influences information cascade dynamics, we compare random graphs with Poisson degree distribution, given by $p_k = \frac{e^{-\langle k \rangle}\langle k \rangle^k}{k!}$, and scale-free power-law degree distribution, $p_k \propto k^{-3}$ [33,34]. Our findings in Fig. 6 reveal intriguing insights into cascade dynamics within these networks.

Panel (A) demonstrates that when both the density of positive links η and the decay factor α are low (e.g., $\eta = 0.2$ and $\alpha = -0.5$), random networks with Poisson degree distribution exhibit greater robustness compared to those with scale-free power-law degree distribution. This is evidenced by smaller cascade sizes (yellow lines), attributed to the homogeneous degree distribution supporting more uniform information diffusion.

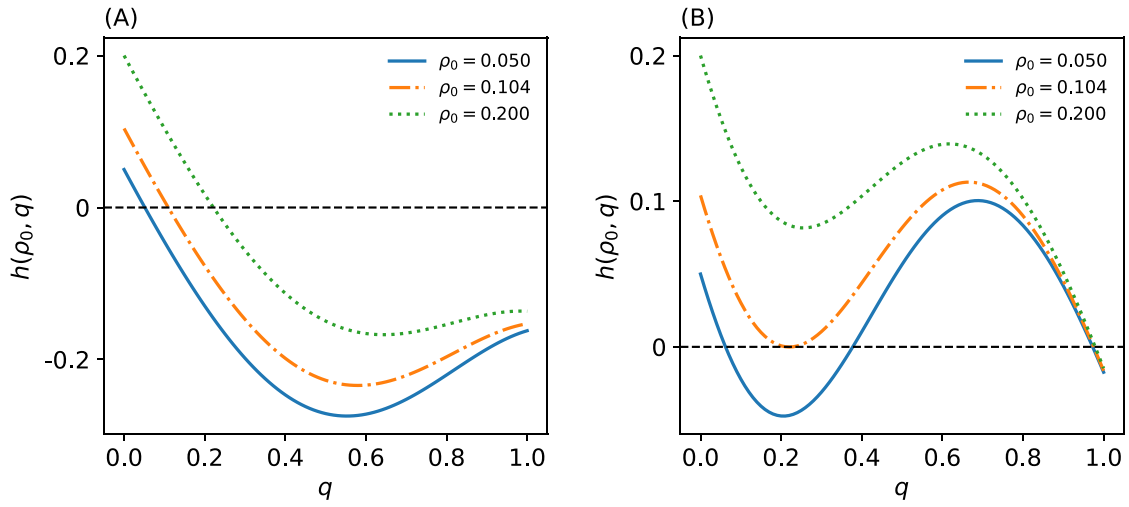

Fig. 4. The graphical solutions of $h(\rho_0, q) = 0$ by varying the seed sizes ρ_0 for different values of α, while maintaining constants $\langle k \rangle = 4$, $\eta = 0.2$, and $\phi = 0.334$. The network employs a Poisson degree distribution $p_k = \frac{e^{-\langle k \rangle}\langle k \rangle^k}{k!}$. Panels (A) and (B) depict the solutions corresponding to $\alpha = 0.5$ and $\alpha = 1$, respectively.

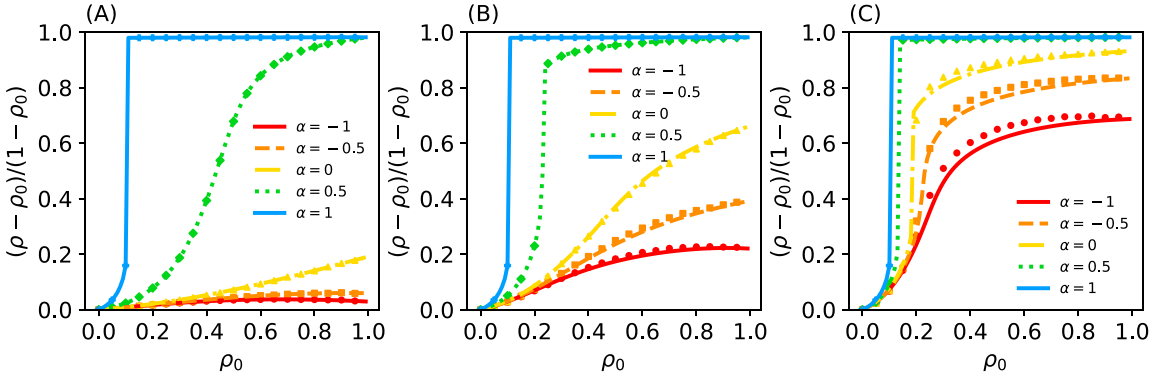

Fig. 5. The figure illustrates the complementary cascade size $(\rho - \rho_0)/(1 - \rho_0)$ as a function of ρ_0 for various values of α. The network employs a Poisson degree distribution $p_k = \frac{e^{-\langle k \rangle}\langle k \rangle^k}{k!}$. The line denotes the analytical results, while the points correspond to the simulation outcomes. The simulation parameters are set as follows: $N = 10^5$, $\phi = 0.334$, and $\langle k \rangle = 4$ with (A) $\eta = 0.2$; (B) $\eta = 0.5$; (C) $\eta = 0.8$. The results are averaged over 100 realizations.

In Panel (A), for higher values of α (e.g., $\alpha = 0.5$), the robustness of Poisson networks relative to scale-free power-law networks depends on the seed size ρ_0. Lower seed sizes ($\rho_0 < 0.3$) show smaller cascade sizes in Poisson networks, indicating greater robustness (green lines). Conversely, higher seed sizes ($\rho_0 > 0.3$) lead to larger cascade sizes, indicating increased fragility compared to scale-free power-law networks (green lines).

Panel (C) highlights that at a very high density of positive links ($\eta = 0.8$), Poisson networks consistently exhibit greater fragility compared to scale-free power-law networks under higher values of ρ_0. The homogeneous structure of Poisson networks facilitates rapid and widespread cascades, making them more susceptible to large-scale information diffusion. In contrast, the heterogeneous structure of scale-free power-law networks, with hubs, localizes and contains information spread, providing greater resilience against cascades (blue lines).

4. Conclusion

This study provides a general framework for exploring information cascades in signed networks, incorporating both positive and negative connections to evaluate their effects on information diffusion. Our findings indicate that negative links can considerably impede the spread of information across networks. We observed that the cascade window diminishes as the density of negative connections increases or their influence becomes weaker. However, as α decreases from 0 to $-\infty$, the cascade window reaches a minimum and remains unchanged. Crucially, our model forecasts under positive α, second-order phase transitions in cascade size with rising network connectivity (measured by average degree), followed by first-order transitions that highlight the difficulties in achieving global cascades in highly interconnected networks. However, for negative α, the relationship between network density and cascade size follows a bell-shaped curve, resulting in two second-order phase transitions in both low and high average degree scenarios. Furthermore, with fixed lower densities of positive links η, and lower weighted parameter α, Poisson networks are consistently more robust compared to scale-free power-law networks. However, this trend reverses when both α and initial seed size ρ_0 are high. Conversely, with a fixed higher density of positive links η, higher ρ_0 makes Poisson networks consistently more robust compared to scale-free power-law networks, while lower ρ_0 makes Poisson networks more fragile.

To further refine our model, several promising directions can be pursued. One approach is to introduce variability in the threshold parameter ϕ and the weighted parameter α across different nodes to capture individual differences in responsiveness and information selection within the network. Another potential extension, inspired by percolation theory, involves the selective removal of negative links. This approach would simulate varying resistance to information spread through negative connections, potentially leading to diverse cascade

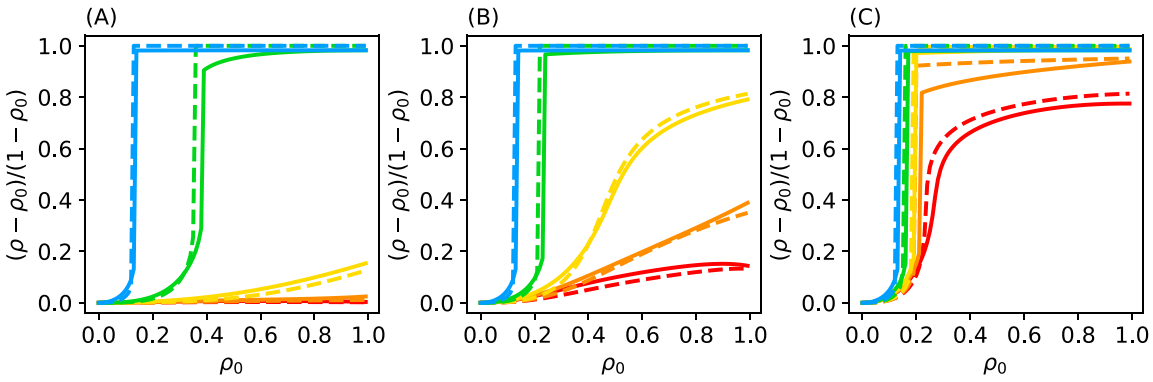

Fig. 6. Complementary cascade size $(\rho-\rho_0)/(1-\rho_0)$ as a function of ρ_0 for various values of $\alpha=-1,-0.5,0,0.5,1$, represented by red, orange, yellow, green, and blue lines respectively, within random networks characterized by Poisson degree distribution $p_k=\frac{e^{-\langle k\rangle}\langle k\rangle^k}{k!}$ (dashed lines) and scale-free power-law degree distribution $p_k\propto k^{-3}$ (solid lines). Solid lines denote analytical results for scale-free power-law networks, while dashed lines correspond to analytical results for Poisson networks. Settings: $\phi=0.334$, $\langle k\rangle=10$, with (A) $\eta=0.2$; (B) $\eta=0.5$; (C) $\eta=0.8$. (For interpretation of the references to color in this figure legend, the reader is referred to the web version of this article.)

dynamics. These proposed modifications aim to deepen our understanding of complex network behaviors and their impact on information cascades.

The implications of our study are profound for both theoretical research and practical applications. By integrating positive and negative interactions within a unified model, we offer a realistic framework for comprehending how information spreads in social networks. This model provides valuable insights into the information cascade dynamics, which are essential for developing strategies to manage information dissemination in real-world contexts.

CRediT authorship contribution statement

Xingfu Ke: Writing – review & editing, Writing – original draft, Visualization, Validation, Methodology. **Youjin Wen:** Visualization, Validation, Methodology. **Hao Yu:** Writing – review & editing, Writing – original draft, Validation, Methodology, Conceptualization. **Fanyuan Meng:** Writing – review & editing, Writing – original draft, Validation, Supervision, Methodology.

Declaration of competing interest

The authors declare that they have no known competing financial interests or personal relationships that could have appeared to influence the work reported in this paper.

Data availability

No data was used for the research described in the article.

Acknowledgments

Our work is supported by the National Natural Science Foundation of China (Grant No. 52374013).

References

[1] Haz Lidice, Acaro Ximena, Guzman Carlos Julio, Espin Luis, Molina Maria Fernanda. Digital platforms as means of social interaction: threats and opportunities in online affective relationships. In: Digital science. Springer; 2019, p. 417–25.

[2] Joo Tang-Mui, Teng Chan-Eang. Impacts of social media (facebook) on human communication and relationships: A view on behavioral change and social unity. Int J Knowl Content Dev Technol 2017;7(4):27–50.

[3] Tang Mui Joo, Chan Eang Teng. The impact of online social networking (social media) on interpersonal communication and relationships. In: Intelligent computing: proceedings of the 2021 computing conference, volume 3. Springer; 2021, p. 624–40.

[4] Bakshy E, Rosenn Itamar, Marlow Cameron A, Adamic Lada A. The role of social networks in information diffusion. In: Proceedings of the 21st international conference on world wide web. 2012.

[5] Guo Yuning, Cao Jianxiang, Lin Weiguo. Social network influence analysis. In: 2019 6th international conference on Dependable Systems and Their Applications. DSA, 2020, p. 517–8.

[6] Lerman Kristina, Ghosh Rumi. Information contagion: An empirical study of the spread of news on digg and twitter social networks. In: Proceedings of the international AAAI conference on web and social media. Vol. 4, 2010, p. 90–7.

[7] Dong Chen, Xu Guiqiong, Yang Pingle, Meng Lei. TSIFIM: A three-stage iterative framework for influence maximization in complex networks. Expert Syst Appl 2023;212:118702.

[8] Zhao Yunwei, Wang Can, Chi Chi-Hung, Lam Kwok-Yan, Wang Sen. A comparative study of transactional and semantic approaches for predicting cascades on Twitter.. In: IJCAI. 2018, p. 1212–8.

[9] Liu Yun, Bao Zemin, Zhang Zhenjiang, Tang Di, Xiong Fei. Information cascades prediction with attention neural network. Hum-Cent Comput Inf Sci 2020;10:1–16.

[10] Chen Zhihao, Wei Jingjing, Liang Shaobin, Cai Tiecheng, Liao Xiangwen. Information cascades prediction with graph attention. Front Phys 2021;9:739202.

[11] Cinelli Matteo, De Francisci Morales Gianmarco, Galeazzi Alessandro, Quattrociocchi Walter, Starnini Michele. The echo chamber effect on social media. Proc Natl Acad Sci 2021;118(9):e2023301118.

[12] Baumann Fabian, Lorenz-Spreen Philipp, Sokolov Igor M, Starnini Michele. Modeling echo chambers and polarization dynamics in social networks. Phys Rev Lett 2020;124(4):048301.

[13] Yang Pingle, Meng Fanyuan, Zhao Laijun, Zhou Lixin. AOGC: An improved gravity centrality based on an adaptive truncation radius and omni-channel paths for identifying key nodes in complex networks. Chaos Solitons Fractals 2023;166:112974.

[14] Buechel Berno, Klößner Stefan, Meng Fanyuan, Nassar Anis. Misinformation due to asymmetric information sharing. J Econom Dynam Control 2023;150:104641.

[15] Acemoglu Daron, Ozdaglar Asuman, ParandehGheibi Ali. Spread of (mis)information in social networks. Games Econom Behav 2010;70(2):194–227.

[16] Vosoughi Soroush, Roy Deb, Aral Sinan. The spread of true and false news online. Science 2018;359(6380):1146–51.

[17] Yu Hao, Xue Bin, Zhang Jianlin, Liu Run-Ran, Liu Yu, Meng Fanyuan. Opinion cascade under perception bias in social networks. Chaos 2023;33(11).

[18] Buechel Berno, Hellmann Tim, Klößner Stefan. Opinion dynamics and wisdom under conformity. J Econom Dynam Control 2015;52:240–57.

[19] Mao Yanbing, Akyol Emrah, Hovakimyan Naira. Impact of confirmation bias on competitive information spread in social networks. IEEE Trans Control Netw Syst 2021;8(2):816–27.

[20] Liu Quan-Hui, Lü Feng-Mao, Zhang Qian, Tang Ming, Zhou Tao. Impacts of opinion leaders on social contagions. Chaos 2018;28(5).

[21] Unicomb Samuel, Iñiguez Gerardo, Karsai Márton. Threshold driven contagion on weighted networks. Sci Rep 2018;8(1):3094.

[22] Li Xiaolin, Wang Peng, Xu Xin-Jian, Xiao Gaoxi. Universal behavior of the linear threshold model on weighted networks. J Parallel Distrib Comput 2019;123:223–9.

[23] Labianca G, Brass Daniel J. Exploring the social ledger: Negative relationships and negative asymmetry in social networks in organizations. Acad Manag Rev 2006;31:596–614.

[24] Meng Fanyuan, Medo Matúš, Buechel Berno. Whom to trust in a signed network? Optimal solution and two heuristic rules. Inform Sci 2022;606:742–62.

[25] Easley David, Kleinberg Jon. Positive and negative relationships. In: Networks, Crowds, and Markets: Reasoning about a Highly Connected World. Cambridge University Press; 2010.
[26] Leskovec Jure, Huttenlocher Daniel, Kleinberg Jon. Signed networks in social media. In: Proceedings of the SIGCHI conference on human factors in computing systems. 2010, p. 1361–70.
[27] He Xiaochen, Du Haifeng, Feldman M, Li Guangyu. Information diffusion in signed networks. PLoS One 2019;14.
[28] Qu Cunquan, Bi Jialin, Wang Guanghui. Personalized information diffusion in signed social networks. J Phys: Complex 2021;2(2):025002.
[29] Hosseini-Pozveh Maryam, Zamanifar Kamran, Naghsh-Nilchi Ahmad Reza. Assessing information diffusion models for influence maximization in signed social networks. Expert Syst Appl 2019;119:476–90.
[30] Watts Duncan J. A simple model of global cascades on random networks. Proc Natl Acad Sci 2002;99(9):5766–71.
[31] Gleeson James P, Cahalane Diarmuid J. Seed size strongly affects cascades on random networks. Phys Rev E 2007;75(5):056103.
[32] Lee Kyu-Min, Lee Sungmin, Min Byungjoon, Goh K-I. Threshold cascade dynamics on signed random networks. Chaos Solitons Fractals 2023;168:113118.
[33] Barabási Albert-László, Albert Réka. Emergence of scaling in random networks. Science 1999;286(5439):509–12.
[34] Barabási Albert-László, Albert Réka, Jeong Hawoong. Mean-field theory for scale-free random networks. Phys A 1999;272(1–2):173–87.